Journal of Applied Mechanics and Technical Physics, Vol. 38, No. 6, 1997

NONLINEAR WAVES IN AN ABSOLUTELY FLEXIBLE FIBER

V. V. Ridel' and M. A. Il'gamov

UDC 534.1

1. Formulation of the Problem and Method of Solution. Oscillating systems having unsymmetrical characteristics of the restoring and external forces are well known. A classical example is a pendulum whose motion is restricted on one side. The mathematical description of these systems contains inequalities, which lead to first-order discontinuities in the coefficients or on the right sides of equations [1]. In the literature, considerable attention has been given to the features of a shock oscillator.

In solid deformable bodies, extended and compressed zones can have different elastic moduli [2]. The dynamic behavior of members made of such materials are covered, for example, in [2–6]. It is shown, in particular, that, along with the set of steady states, which depend only on the initial conditions, there are subharmonic resonances. They can be accompanied by a cascade of bifurcations of period doubling.

In this work, we analyzed a model in which the inequality in the physical law leads to a change in the type of differential equation of motion. We established a number of features that are not studied, in the author's opinion, in the theory of nonlinear oscillations and waves.

We study longitudinal oscillations of a previously extended, forward, viscoelastic fiber whose one end is immovable and the other vibrates along the fiber by a harmonic law. Energy dissipation depends on the presence of physical viscosity in the material, which is described by the Kelvin–Voigt model. The main feature of the problem is the absolute flexibility of the fiber, which implies that it cannot resist compression (the force in it cannot be negative).

The wave process in the viscoelastic fiber is described by the following system of equations in dimensionless form:

$$\frac{\partial u}{\partial t} = \frac{\partial N}{\partial s}, \qquad \frac{\partial \varepsilon}{\partial t} = \frac{\partial u}{\partial s}; \tag{1.1}$$

$$N = \begin{cases} f(\varepsilon, \dot{\varepsilon}), & f \geqslant 0, \\ 0, & f < 0; \end{cases} \tag{1.2}$$

$$f = \varepsilon + \dot{\eta}\varepsilon, \quad \varepsilon = \partial x/\partial s - 1, \quad \partial x/\partial s \geqslant 0. \tag{1.3}$$

Here the velocity u is related to the velocity of the longitudinal elastic wave, the coordinates (x is the Eulerian coordinate and s is the Lagrangian coordinate) are related to the length of the fiber and N is related to the elastic modulus, ε is the strain, and $(\dot{}) \equiv \partial/\partial t$. The inequality in (1.3) ensures nonpenetration of neighboring points of the fiber through one another. The boundary and initial conditions of the problem are of the form

$$x(0,t) = -p\sin\omega t, \qquad x(1,t) = 1 + \varepsilon_0; \tag{1.4}$$

$$x(s,0) = s(1+\varepsilon_0), \qquad u(s,0) = 0 \quad (s > 0), \tag{1.5}$$

where ε_0, p, and ω are the initial tensile strain of the fiber and the amplitude and angular frequency of oscillations of its left end.

Institute of Mechanics and Mechanical Engineering, Kazan' Scientific Center, Russian Academy of Sciences, Kazan' 420111. Translated from Prikladnaya Mekhanika i Tekhnicheskaya Fizika, Vol. 38, No. 6, pp. 139–146, November–December, 1997. Original article submitted August 17, 1995; revision submitted May 23, 1996.

 0021-8944/97/3806-0936 $18.00

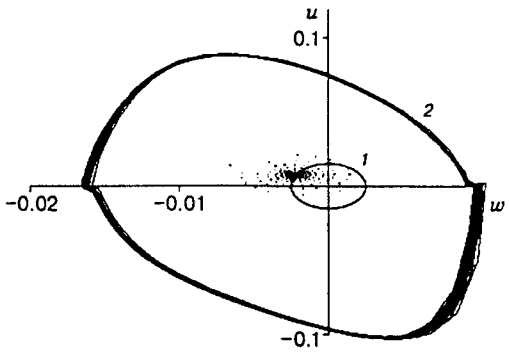

Fig. 1

The nonlinearity of system (1.1)–(1.5) is due to inequality (1.2). When $N = f(\varepsilon, \dot{\varepsilon})$ and there is no restriction on the sign of f in condition (1.2), the problem reduces to the well-know equation of longitudinal oscillations of a viscoelastic bar:

$$\frac{\partial^2 x}{\partial t^2} - \frac{\partial^2 x}{\partial s^2} - \eta \frac{\partial^3 x}{\partial x^2 \partial t} = 0. \tag{1.6}$$

In this case, the natural frequencies and the damping coefficients are of the form

$$\omega_m = m\pi\sqrt{1 - (\eta m\pi/2)^2}, \qquad \delta_m = (1/2)\eta m^2\pi^2 \quad (m = 1, 2, \ldots). \tag{1.7}$$

System (1.1)–(1.5) was integrated using a numerical algorithm based on an explicit difference scheme. The algorithm was tested in calculations of unsteady processes in soft shells [7]. In each time layer, we analyze the type of stressed state in all elements of a discrete region of a fiber. If somewhere $f < 0$, the force N in the corresponding element is set to zero without changing its strain. For solutions with a continuous second derivative, the difference scheme is of second-order approximation for τ and h and is stable with satisfaction of the conditions [8]

$$0.5 - \sqrt{0.25 - \beta} < \tau/h < 0.5 + \sqrt{0.25 - \beta}, \quad \beta = \eta\tau/h^2 < 0.25.$$

The practical convergence of the solution of the nonlinear problems with refinement of h was determined by numerical experiments.

The transition process and the steady motion regime are described using several control points (nodes of the difference grid). For them, we constructed the Poincaré transform $X_n = X(t_0 + nT)$ $(n = 0, 1, 2, \ldots)$ and the projections of the phase trajectories onto the plane (w, u), where w is the displacement of the point from the equilibrium position at $t = 0$ and $T = 2\pi/\omega$ is the period of external action. Next, we consider steady oscillation regimes after multiple reflection of waves from the ends of the fiber.

2. Oscillations of a Viscoelastic Bar and the Fiber. To estimate the effect of condition (1.2) on the wave process, we compare the solutions of two problems: in one of these, inequalities (1.2) are ignored, i.e., $N \equiv f$, and, in the other, they are taken into account. In both variants, it is assumed that $\omega = 6$, $\eta = 0.003$, and $p = 0.005$.

In the first case, we have the linear problem (1.4)–(1.6) for a viscoelastic bar. After the attainment of a steady regime, oscillations proceed with the period of external action. In this case, the Poincaré section is a stationary point. The phase trajectory enters the limiting cycle in the form of an ellipse (Fig. 1, curve 1). Here the results for the middle point ($s = 0.5$) in the time interval $100T$ for $\omega = 6$ are given. The force distribution is of the form of a standing wave with two nodes and compression zones. This numerical solution agrees well with the analytical solution of [9–11].

If conditions (1.2) are taken into account, the character of the wave process changes radically. The phase trajectories are not smooth (Fig. 1, curve 2). They have angular points and straight segments. The force distribution along the fiber is of the form of a traveling tension wave (Fig. 2a) The results are given

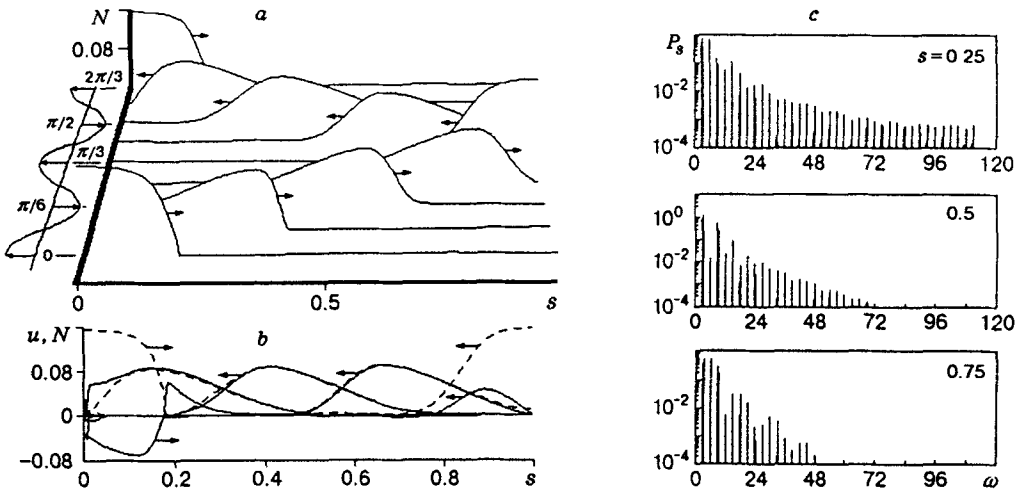

Fig. 2

at equal intervals $\Delta t = T/4 = \pi/12$ for $\omega = 6$. The variation in the velocity of the left end of the fiber in the interval $2T = 2\pi/3$ is shown schematically along the time axis. The arrow shows the direction of wave propagation. Immediately after reflection from one of the ends, the leading edge of the wave moves toward the unstressed zone, decreases in amplitude, and levels out. Note that, in the previously extended fiber, unstressed zones occur after the first reflection of waves from the fiber ends.

Figure 2b compares the tension waves N and the velocity waves u (the dashed and solid curves, respectively). The shapes of steady waves are shown at equal time intervals $T/4$ at moments after the reflection from the right fixed end, where $u = 0$ and the tension is maximal. The wave propagation direction is shown by arrows. Characteristically, in what follows, the tension and velocity waves coincide in both shape and intensity. This is the case up to the moment the front reaches the let end of the fiber. After reflection, the sign of the velocity is reversed, as shown by arrows in Fig. 2b. In motion to the right, the tension and velocity waves again have identical shapes but opposite signs (not shown in the figure).

Figure 2c shows the power spectra P_s at three points. The angular frequency of velocity fluctuations at these points is plotted on the abscissa. Note the following features:

(1) the spectrum is discrete for all resonance frequencies (this is discussed in detail below);

(2) oscillations with a wider spectrum occur near the excitation source ($s = 0.25$) and oscillations with a less wide spectrum occur near the right end;

(3) at the middle of the fiber, the power of the oscillations at frequency $\omega = 6$ is about two times lower than at neighboring frequencies, although excitation occurs precisely at this frequency.

The effect of physical viscosity was analyzed for $\omega = 4$, $p = 0.005$, and $0.002 < \eta < 0.003$. For the coefficient $\eta = 0.002$, the system enters a subharmonic oscillation regime with a period $8T$ (in the steady motion regime there are four pairs of stationary points present in the Poincaré section). In the range $0.0025 < \eta < 0.003$, the system has the limiting cycle with a period T. However, for the range $0.002 < \eta < 0.0025$, no period-doubling cascade was observed. Thus, there is a strong dependence of the solution on the dissipative term. This issue requires further investigation.

3. Dependence of the Waves on the Excitation Frequency and Initial Tension of the Fiber. We study the occurrence of nonlinear waves in the fiber with increase in the excitation frequency from $\omega = 1$ (for $\varepsilon_0 = 0.02$, $\eta = 0.003$, and $p = 0.005$).

Figure 3 shows the phase portrait for the middle point of the fiber in the time interval of $100\,T$ at excitation frequencies $\omega = 1$, 2, and 3. The initial strain ε_0 increases the average tension in the fiber, about which fluctuations of forces occur. In this connection, the condition $f > 0$ is not violated for $\omega = 1$ and 2. The fiber behaves as a viscoelastic bar, whose oscillations are of the form of a standing wave. As ω approaches the

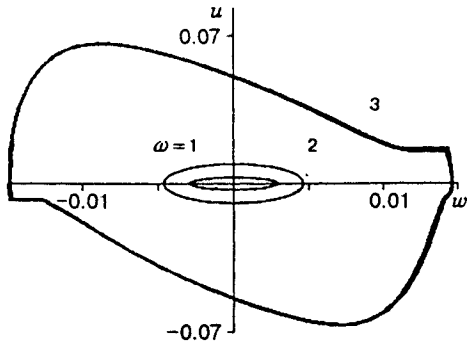

Fig. 3

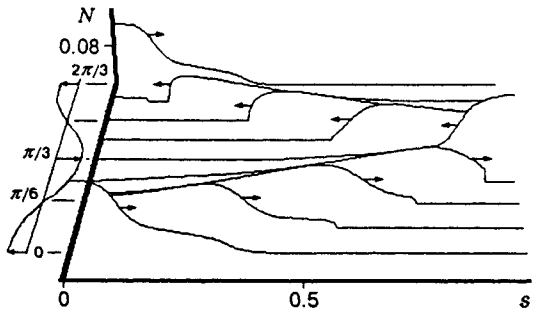

Fig. 4

first natural frequency ω_1, determined from (1.7), the amplitude increases suddenly. As the rarefaction wave reaches the value $f < 0$, condition (1.2) becomes true, according to which the values of N are set to zero. In the fiber, an unstressed zone appears, moves, disappears, and again appears with time.

Thus, the standing linear wave becomes a traveling nonlinear wave with steep edges (Fig. 4). The figure shows the pattern for $\omega = 3$ and $\Delta t = T/8 = \pi/12$ in the time interval $T = 2\pi/3$. The phase portrait for $\omega = 3$ changes suddenly (see Fig. 3). The amplitudes of the oscillations considerably increase. Angular points and horizontal portions of the trajectories ($u = \text{const}$) appear, which indicate a discontinuity of the phase velocity and the passage of the unstressed zone through the given point of the fiber.

In the Poincaré section at $\omega = 1$ and 2 there is a stable focus, which corresponds to the limiting cycle in Fig. 3. At an oscillation frequency $\omega = 3$, which is close to the resonance frequency, a dense accumulation of points occurs in the Poincaré section. This motion can be only approximately considered periodic with a frequency $\omega = 3$. Accordingly, instead of the limiting cycle, there is a rather dense bundle of phase trajectories (see Fig. 3).

Note that, for dimensionless excitation frequencies ω of 1 to 15, the curve of maximum tension at the point $s = 0.25$ has five peaks which correspond to resonances (Fig. 5). The resonance frequencies are divisible by 3, whereas the natural frequencies from (1.7) are divisible by π [the square root in (1.7) differs little from unity]. The difference can be explained by the simultaneous effect of unstressed zones that arise and viscosity on the wave process (on the decrease in the wave-propagation velocity) in the nonlinear problem. In particular, the unstressed zones of the fiber show only the mass characteristic in the absence of elastic forces. Characteristically, all resonances, except for the first, have equal intensity, although, with increase in the excitation frequency, the velocity of the left end of the fiber (the factor of oscillation excitation) increase proportionally. For points with the coordinates $s = 0.5$ and $s = 0.75$, this saturation occurs at higher resonance frequencies.

The dimensionless value of the initial tension of the fiber ε_0 is also given in Fig. 5. The frequency ω_0 that corresponds to the point of intersection of the curve with the horizontal line $N = \varepsilon_0$ is the threshold frequency. At $\omega < \omega_0$, standing waves occur in the fiber, as in the bar, as noted above (for $\omega = 1$ and 2). At $\omega > \omega_0$, nonlinear waves arise. The threshold frequency ω_0 depends on the initial tension ε_0 and the other parameters of the problem. Evidently, for unchanged parameter values, an increase in the initial tension leads to the occurrence of frequency ranges in which intense traveling waves (in the vicinity of resonances) and standing waves (far from the resonance zones) are excited.

We consider the behavior of the system at constant excitation frequency and gradually decreased initial tension (in experiments, this can be achieved by slow release of the right end of the fiber). We assume that $\varepsilon_0 = 0.06$ and $\omega = 4$.

Figure 6 shows curves of the tension distribution in the fiber at time intervals of $T/4$. Under these conditions, as can bee seen from Fig. 6a, standing waves with an amplitude of ≈ 0.024 and one node at the

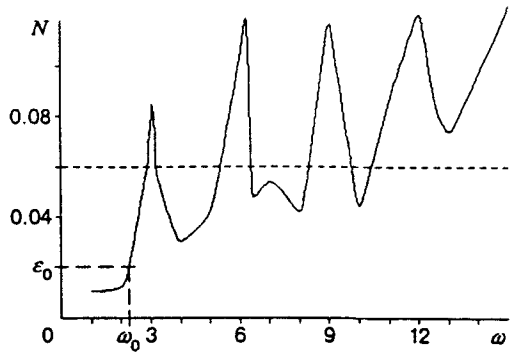

Fig. 5

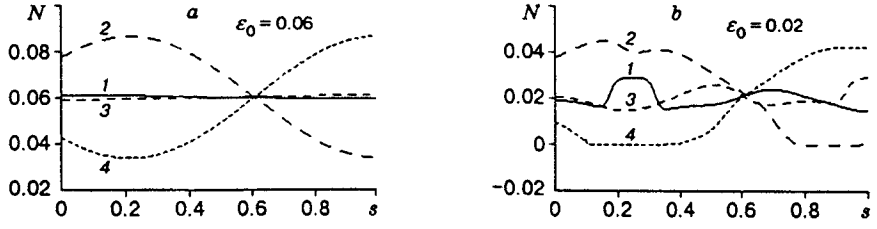

Fig. 6

point $s \approx 0.6$ are excited. This pattern remains unchanged with increase in ε_0 to 0.024. However, a further decrease in the initial tension ($\varepsilon_0 = 0.02$ in Fig. 6b) leads to strong distortions, characterized by a complex combination of standing and traveling waves.

If we consider the excitation frequency in the vicinity of a resonance, for example, at $\omega = 3$, an increase in ε_0 from 0.06 to 0.02 does not affect the character of traveling waves in the fiber (see Fig. 4) but only decreases their intensity. The corresponding phase trajectories remain similar to one another, but decrease in dimensions to the value shown in Fig. 3.

4. Wave Excitation Regime at Resonance Frequencies. Two oscillation regimes can be distinguished in the system, depending on the excitation frequency. Thus, at $\omega = 3$ and 6, we observe a resonance regime for which the steady wave process is shown in Figs. 2 and 4. It is evident from the figures that the motion of the left end of the fiber gives rise to a single pulse, which moves along the unstressed fiber. With increase in ω, the pulse intensity increases and its length decreases, but the pulse velocity practically does not depend on the excitation frequency. This effect leads to a constant oscillation period of the system at oscillation frequencies close to the resonance frequencies. If the directions of wave propagation and the velocity of points ahead of the front coincide, the front becomes steeper, otherwise, it flattens out.

A specific feature of the process is that the motion of the left end of the fiber changes the pulse intensity only when the stressed zone is in the vicinity of the vibrating end point. Otherwise, its motion at the left end can affect only the nearest points upon their direct contact during collapse of the fiber, according to condition (1.3). The remaining points in the unstressed zone move uniformly at a velocity they had at the moment when the forces in the vicinity of these points were set to zero.

We consider in detail the time history for the excitation of waves at a resonance frequency $\omega = 9$. Figure 7 shows the velocity and tension values at the point $s = 0.75$. Here the time axis is the same for both plots. The above coincidence of the velocity and tension waves is clearly seen. In this case, the waves that move to the right have a higher intensity than the waves that move in the opposite direction. This is explained by the unsymmetric boundary conditions at the ends of the fiber.

For the excitation at a frequency $\omega = 6$, small waves appear between the main waves. As noted above, at lower excitation frequencies they are absent. At $\omega = 9$, 12, and 15, the indicated small waves are enhanced.

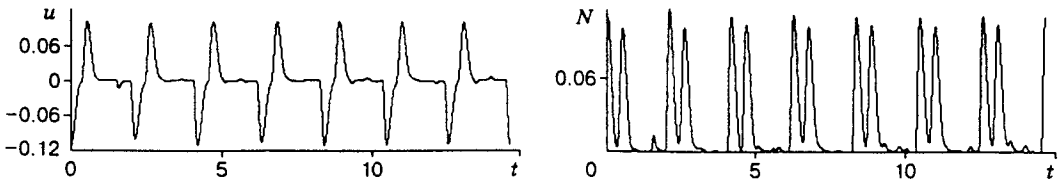

Fig. 7

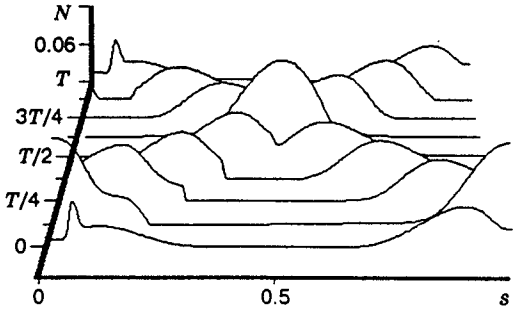

Fig. 8

This is explained by the interaction of the motion of the end and unstressed zones in the fiber as the velocity of the left end of the fiber increases at higher frequencies. It should be noted that the power spectrum for excitation at resonance frequencies have the feature indicated in Fig. 2c: the spectral density of oscillations of fiber points at a frequency of 3 is always much higher than the corresponding values at frequencies that coincide with the perturbing frequency.

Thus, at excitation frequencies divisible by 3 ($\omega = 3m$, $m = 1, \ldots, 5$), a resonance regime occurs and the oscillations can be considered periodic with a constant period $T_{\text{system}} = 2\pi/3$. In this case, each value of m corresponds to the m-cycle $T_{\text{system}} = mT$, because in the Poincaré section in the phase plane (w, u), m dense accumulations of points are observed.

5. Wave Excitation Regime at Nonresonance Frequencies. At frequencies that are fairly distant from the resonance frequencies, the system rapidly enters the limiting cycle with a period of external action T or with a period divisible by it.

Figure 8 shows the spatial-temporal pattern of tension for excitation at a frequency $\omega = 6.2$. Since this excitation region is behind the second resonance (see Fig. 5), two waves that move on two halves of the length and collide at the middle of the fiber are observed. This pattern is more usual in the theory of nonlinear waves [11, 12]. The oscillations at each point are subharmonic with a period $5T$. The phase trajectories form a pentacycle. The highest spectral density corresponds to the excitation frequency.

6. Conclusions. The analysis performed reveals the effect of previous tension and excitation frequencies on the longitudinal oscillations of the fiber. The amplitude of displacements of one end of the fiber was assumed to be constant (the other end was fixed).

Depending on the level of previous tension, the motion of the fiber can be represented by both standing and traveling waves. The first type of oscillations is realized when the tensile forces excited by the source do not exceed the previous tensile forces. Otherwise, a complex combination of standing and traveling waves occurs or only traveling waves occur. The latter have a number of features, among which are their higher intensity compared with the intensity of standing waves, the occurrence of moving unstressed zones, the nondependence of the oscillation frequencies on the excitation frequency (near resonances), and a decrease in wave-propagation velocity and resonance frequencies. The latter is explained by the contribution of unstressed zones, in which only mass forces act, to the motion. The constant-frequency oscillation regime at various excitation frequencies is due to the selective interaction of the moving end of the fiber with stressed and unstressed zones.

This work was partially supported by the International Science Foundation (Grant No. RH4000).

REFERENCES

1. Yu. I. Neimark, *Method of Point Images in the Theory of Nonlinear Oscillations* [in Russian], Nauka, Moscow (1972).
2. S. A. Ambartsumyan, *Different-Modulus Theory of Elasticity* [in Russian], Nauka, Moscow (1982).
3. G. Tee, "Periodic oscillations of a bilinear oscillator, with reference to moored marine systems, *Phys. Fluids*, **25**, No. 6, 936–941 (1982).
4. J. M. T. Thompson, "Subharmonic resonance of a bilinear oscillator with applications to moored marine systems," *J. Appl. Math.*, **31**, No. 3, 207–234 (1983).
5. L. N. Virgin, "On the harmonic response of an oscillator with unsymmetric restoring force," *J. Sound Vibr.*, **126(1)**, 157–165 (1988).
6. L. A. Ostrovsky, "Nonlinear dynamics of media with complex structures," *Dynam. Systems*, No. 1, 115–130 (1993).
7. V. V. Ridel' and B. V. Gulin, *Dynamics of Soft Shells* [in Russian], Nauka, Moscow (1990).
8. A. A. Samarskii and Yu. P. Popov, *Difference Methods of Solution of Gas-Dynamic Problems* [in Russian], Nauka, Moscow (1980).
9. S. P. Timoshenko, D. H. Young, and W. Weaver, *Oscillation Problems in Engineering*, Wiley, New York (1975).
10. Kh. A. Rakhmatulin and Yu. A. Dem'yanov, *Strength under Intense Short-Term Loading* [in Russian], Fizmatgiz, Moscow (1961).
11. M. I. Rabinovich and D. I. Trubetskov, *Introduction to the Theory of Oscillations and Waves* [in Russian] , Nauka, Moscow (1992).
12. A. I. Potapov, *Nonlinear Deformation Waves in Bars and Plates* [in Russian], Gor'kii Univ., Gor'kii (1985).